Stability Analysis of a Multi-Camera Photogrammetric System used for Structural Health Monitoring

Ivan DETCHEV, Canada; Ayman HABIB, United States; and Derek LICHTI, Canada

Key words: Digital Close Range Photogrammetry; Geometric Camera Calibration; Camera Stability Analysis; Multi-Sensor Systems

SUMMARY

Multi-camera photogrammetric systems are becoming more and more widespread due to the off-the-shelf availability of inexpensive digital cameras. Such systems are employed in a variety of metric applications including mobile mapping, vision-aided navigation, biomedical engineering, and structural deformation monitoring. In order to meet desired precision specifications these systems should be calibrated on a regular basis. The calibration parameters to be solved for include both the interior orientation parameters of each camera, and the mounting parameters of each camera with respect to a reference camera. The frequency of such system calibration depends on the build quality of the system components and on any external forces related to the environment in which the system is being used. Since stability over time has been recognized as a major factor for metric quality in sensors used for photogrammetric work, it is necessary to investigate how often a particular system should be calibrated. This could be achieved through a system stability analysis where the impact on the photogrammetric reconstruction of any changes in the calibration parameters can be quantified.

A numerical tool for checking the variations of both the internal geometry and the mounting parameter of each camera in a system was developed. This paper presents three methods that could be used for the system stability analysis of a multi-camera photogrammetric system. All methods are based on an image space synthetic grid, and provide measures of (in)stability in terms of image space units. The methods were tested with both simulated and real world data. Based on the simulation, the best of the three methods was chosen in the most general case. Given the real system calibration data for two particular system setups in a structural laboratory, the developed system stability tool could be used to either make recommendations on the frequency of calibration and/or identify the sources of instability.

Stability Analysis of a Multi-Camera Photogrammetric System used for Structural Health Monitoring

Ivan DETCHEV, Canada; Ayman HABIB, United States; and Derek LICHTI, Canada

1. INTRODUCTION

Current close range photogrammetric systems consist of arrays or clusters of digital cameras. Those cameras are rigidly mounted to a stationary or a moving platform. In order to achieve precise 3D reconstruction of the object space of interest, the multi-camera system must be correctly calibrated. Applications where such a correct system calibration is necessary include direct sensor orientation in mobile mapping (Rau et al., 2011), dense matching for full surface reconstruction (Remondino et al., 2008), infrastructure health monitoring (Detchev et al., 2013; Kwak et al., 2013), motion capture or other metric biomedical engineering applications (Detchev et al., 2011; Lichti et al., 2015), multi-sensor integration (Tommaselli et al., 2013), underwater photogrammetry (Harvey and Shortis, 1996), etc. Desirably, a photogrammetric system should be calibrated before and after each deployment. However, this may not be always feasible. So the frequency of calibration for a particular photogrammetric system must be investigated for the specific environment it is being used in. This investigation can be accomplished through a methodology called system stability analysis (Habib et al., 2014).

This article provides important background information on photogrammetric system calibration and stability analysis. It then briefly presents three methods to be used for stability analysis of multi-camera systems. The methodologies and their related hypotheses are tested using both simulated data and also using real calibration data. The actual calibrations were performed for a system set up in a structural laboratory where sub-millimetre level deflections must be measured. The objectives of this paper are to select which system stability method is the most appropriate in general, and how often should the photogrammetric system be calibrated given the busy environment and wide scope of experiments performed in the lab.

2. BACKGROUND

This section gives brief background information on three aspects of quality assurance measures used in photogrammetric applications: system design, calibration, and stability analysis. Both the calibration of an individual camera and system calibration are reviewed as well as the stability analysis of a single camera and the one of a multi-camera system.

2.1 Photogrammetric system design

A photogrammetric system typically includes multiple digital cameras. The cameras may be mounted on a stationary or a moving platform, and the object(s) of interest may also be either stationary or moving. In this research work, the use of a photogrammetric system is intended on a stationary platform in a laboratory setting, where the objects of interest are experiencing dynamic deflections. In order for the photogrammetric system to yield good quality images and for the reconstruction to work, the camera settings must be configured for a specific integration time and the shutter releases must be synchronized.

2.2 Photogrammetric system calibration

In addition to the camera configuration and synchronization requirements, in order for the 3D photogrammetric reconstruction to be accurate, a photogrammetric system calibration must also be performed. The system calibration can be performed in-situ or in an indoor lab with a 2D or 3D test field. The two aspects of the calibration, i.e., estimating the interior orientation parameters (IOPs) and estimating the camera mounting parameters (CMPs), are listed next.

2.2.1 Interior orientation parameters

Estimating the IOPs for each of the involved cameras in the system is also known as geometric camera calibration. This is especially crucial for inexpensive off-the-shelf digital cameras, which are not designed and built for precise engineering work (Fraser, 1997; Habib and Morgan, 2003). The IOPs of interest usually are the principal distance (c), the principal point offset (x_p, y_p), the appropriate distortion parameters necessary to describe deviations from the collinearity model (e.g., $k_1, k_2, k_3, p_1, p_2, a_1, a_2$). In this project specifically the distortion parameters used are k_1, k_2, p_1 and p_2. The IOPs are typically estimated via a self-calibrating bundle adjustment.

2.2.2 Camera mounting parameters

Estimating the CMPs refers to estimating of the position and orientation of each camera with respect to a reference camera. The positional component or the lever arm is a 3D vector and can be annotated as $r_{c_k}^{c_r}$, where c_k is a particular camera in question and c_r is the reference camera. It includes the spatial offsets b_X, b_Y, and b_Z.The rotational component or the boresight is a 3x3 matrix and can be annotated as $R_{c_k}^{c_r}$. The elements of this matrix are functions of the angular offsets b_ω, b_φ, and b_κ. There are a few methods for estimating the CMPs. The method chosen here is referred to as a bundle adjustment with built-in relative orientation constraints (ROCs) (Rau et al., 2011). In fact, the estimation of the CMPs is combined with the one for the IOPs in a simultaneous self-calibrating bundle adjustment, and is performed in-situ.

2.3 Photogrammetric stability analysis

While the system calibration quality assurance measures in the photogrammetric reconstruction process are well addressed in literature, the concept of photogrammetric stability analysis is often neglected. Stability analysis is especially important in the context of a photogrammetric system consisting of multiple cameras where the calibration is performed with the built-in ROCs model. This portion of the paper explains the issue of stability analysis of a single camera, and extends it to the multi-camera system scenario.

2.3.1 Stability analysis of a single camera

Calibrating a camera once does not guarantee that the estimated IOPs will be valid at the time of actually employing the camera in a data acquisition campaign. Variations in the internal geometry of a camera over time could be intentional (e.g., due to the mode of operation such as focusing the lens for every acquired photo) or unintended (e.g., the structural instability of the camera causes mechanical movements, or cannot handle routine use, transportation, disassembly, reassembly, or other external forces or effects) (Habib et al., 2014). Variations in the IOPs could occur in the course of a single data collection campaign. Since they are at the photo level, those variations are called "photo invariant" (Shortis et al., 1998). Variations in the IOPs could also occur between different data collection campaigns. Since they are at the block level, those variations are called "block invariant" (Shortis et al., 1998). In general, there could be three camera (in)stability scenarios (also summarized in Table 1):

a) No instability – photos within the same block and different blocks use the same set of IOPs (see Figure 1a); this is the most desirable scenario for precise photogrammetric work;
b) Instability between different blocks – while photos within each block can use the same IOPs, different IOPs must be used for the different blocks (see Figure 1b); this scenario is acceptable as long as the camera is calibrated for every different block;
c) Instability within a block – each photo exhibits significantly different IOPs (see Figure 1c); this is an undesirable scenario for photogrammetric work.

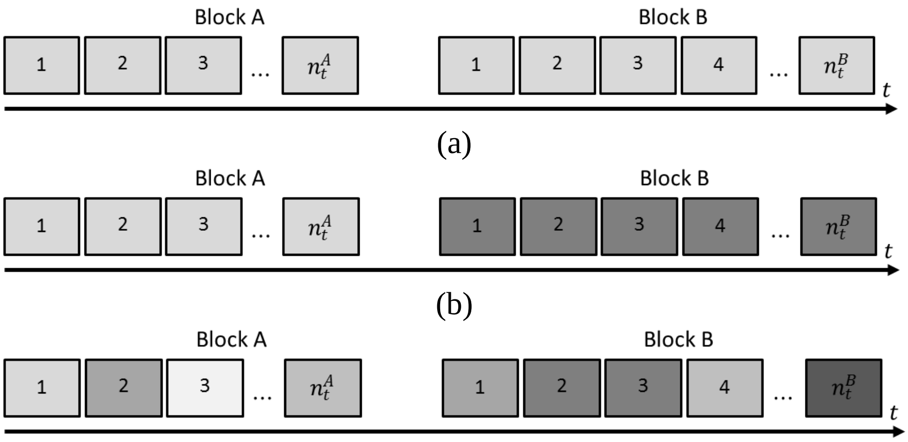

(c)

Figure 1: Examples of no instability (a), instability between different blocks (b), and instability within a block (c) (after Habib et al. (2014))

Table 1: Summary of the types of stability scenarios for a single camera

Photo level / block level	Stable, different blocks are invariant	Unstable, different blocks are variant
Stable, photos within a block are invariant	a) Most desirable	b) Acceptable, but requires re-calibration
Unstable, photos within a block are variant	N/A	c) Not desirable

There are two approaches for coping with geometric instability of a camera. One of them is through a parametrization, and the other one is through a mechanical stabilization (Rieke-Zapp et al., 2009). For metrology applications such as the measurement of deflections in concrete beam specimens, it is recommended to perform the latter. For example, fixing the zoom and focus rings of the lens, and turning off any product features that counteract photogrammetric uses (e.g., auto focus, auto sensor dust removal, and auto lens movement for blur reduction).

The stability of the internal geometry of a camera must also be assessed. Such camera stability analysis could help decide on the frequency of any necessary re-calibrations (Shortis and Beyer, 1997). There are two approaches to performing such camera stability analysis. One is based on statistical testing (Shortis and Beyer, 1997) and a separate procedure involving control data for assessing the impact of any instability on the reconstruction results is necessary (Shortis et al., 2006, 2001). The other approach for camera stability analysis is based on image (Habib et al., 2005; Habib and Morgan, 2005) or object space simulations (Lichti et al., 2009). The advantage of the simulation-based stability analysis methods is that they not only assess the stability of a camera, but also provide a measure of equivalency between two sets of IOPs without using any control data. Note that the simulation-based methods also do not require any knowledge of the variance-covariance matrix of the estimated system calibration parameters.

2.3.2 Stability analysis of a multi-camera system

The (in)stability scenarios depicted in Figure 1 and summarized in Table 1 could also be extended from a single camera case to a multi-camera system case where the photo (or camera) level of stability is now a level of an ensemble of photos (cameras). That is, in the multi-camera system case, of interest is not only the stability of the IOPs of the individual cameras, but also the stability of the involved CMPs. The most straight forward way of performing system stability analysis is by simultaneously comparing two sets of IOPs and two sets of CMPs at a time. For example, if camera stations c_i and c_j are part of the system in question, it must be shown whether the cumulative effect on the reconstruction process of two sets of IOPs (i.e., $IOP_i(t_1)$ and $IOP_j(t_1)$ vs. $IOP_i(t_2)$ and $IOP_j(t_2)$) and two sets of CMPs (i.e., $r_{c_j}^{c_i}(t_1)$ and $R_{c_j}^{c_i}(t_1)$ vs. $r_{c_j}^{c_i}(t_2)$ and $R_{c_j}^{c_i}(t_2)$) is equivalent or not (see Figure 2).

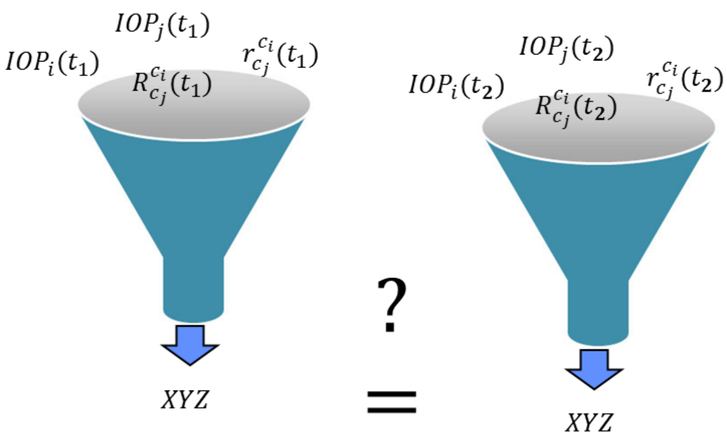

Figure 2: Conceptual illustration of the stability analysis for two cameras (Detchev et al., 2015)

Performing system stability analysis based on statistical testing was addressed in Harvey and Shortis (1998) and Shortis et al. (2000), while the one based on image space simulation was introduced for the first time in Habib at al. (2014). For the sake of completeness, the methodology of the latter approach is briefly re-explained in the next section of the paper.

3. METHODOLOGY FOR SYSTEM STABILITY ANALYSIS

In this section, three methodologies for the simultaneous comparison of two IOP sets and two CMP sets are concisely presented. Note that the article by Habib et al. (2014) should be read for more details. Similarly to the previously reviewed stability analysis methodologies for a single camera or methods used for other sensors (Lichti, 2008), the presented methodologies for system stability analysis are simulation-based. Note that the term "simulation-based" only refers to the fact that a synthetic grid in image space is used for evaluating the stability of the system calibration parameters. The system calibration parameters being tested could be real, not necessarily simulated. The methodologies have the following structure:

- A synthetic regular grid is defined in the image space of one of the cameras, c_i;
- The IOPs and the CMPs of this camera from the first calibration session are used to remove the distortions at the grid vertices and compute the object space coordinates of each vertex by forward projecting them to a range of plausible object space depths;
- The image space coordinates of the grid points for the other camera, c_j, are computed by backward projection using its IOPs and the CMPs from again the first calibration session; this is done for all depth ranges;
- The effect of having different IOPs and CMPs from another calibration session is estimated in image units for all simulated points and all depth levels using one of the methodologies (to be presented in the next three sub-subsections); and
- The RMSE value for all the differences/offsets is compared to the expected image space coordinate measurement precision; if the RMSE value is the smaller one, then the system is deemed stable, and if the RMSE value is the greater one, the system would be considered unstable.

The three methodologies for the system stability analysis are: (1) combination of forward and backward projections; (2) object space parallax in image units; and (3) variation in the normalized image coordinates. They are explained in the next three sub-subsections.

3.1 Method 1: combination of forward and backward projections

In this method, the grid of points from one camera, c_i, is first forward projected to the object space with one set of system calibration parameters. The object space coordinates are then backward projected to the image space of the other camera, c_j, using the two different sets of system calibration parameters (see Figure 3).

The RMSE values for the x and y components can be computed based on the differences shown in Equation (1):

$$\delta x_m = x_m^{c_j}(t_1) - x_m^{c_j}(t_2) \qquad \delta y_m = y_m^{c_j}(t_1) - y_m^{c_j}(t_2) \tag{1}$$

It should be noted that any changes in the IOPs for the first camera are not considered in this system stability analysis method. Ignoring such a variation would be acceptable as long as the system instability is mainly assumed to arise from changes in the CMPs (i.e., lever arm components and boresight angles) relating the camera stereo pairs.

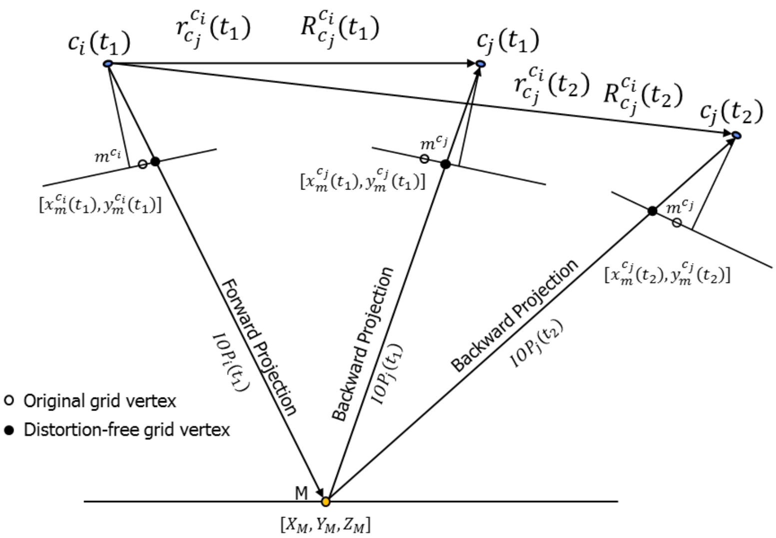

Figure 3: Illustration of method 1 (combination of forward and backward projections) (Habib et al., 2014)

3.2 Method 2: object space parallax in image units

In this method, of interest is evaluating the x parallax (i.e., what defines the object shape or the camera to object depth) and the y parallax (i.e., what makes the image matching process more difficult and the 3D reconstruction results less precise) for the pair of cameras. This is accomplished by quantifying the object space discrepancy arising from the variations in the IOPs and CMPs for both cameras (see Figure 4). This object space discrepancy is decomposed into X and Y components within an object space decomposition plane. The resultant D_X (parallel to baseline) and D_Y (perpendicular to baseline) components are then scaled to image units using the average principal distance, $\bar{c}$, and the object space depth, Z (see Equation (2)). The RMSE for the x and y components is computed based on the differences shown in Equation (2):

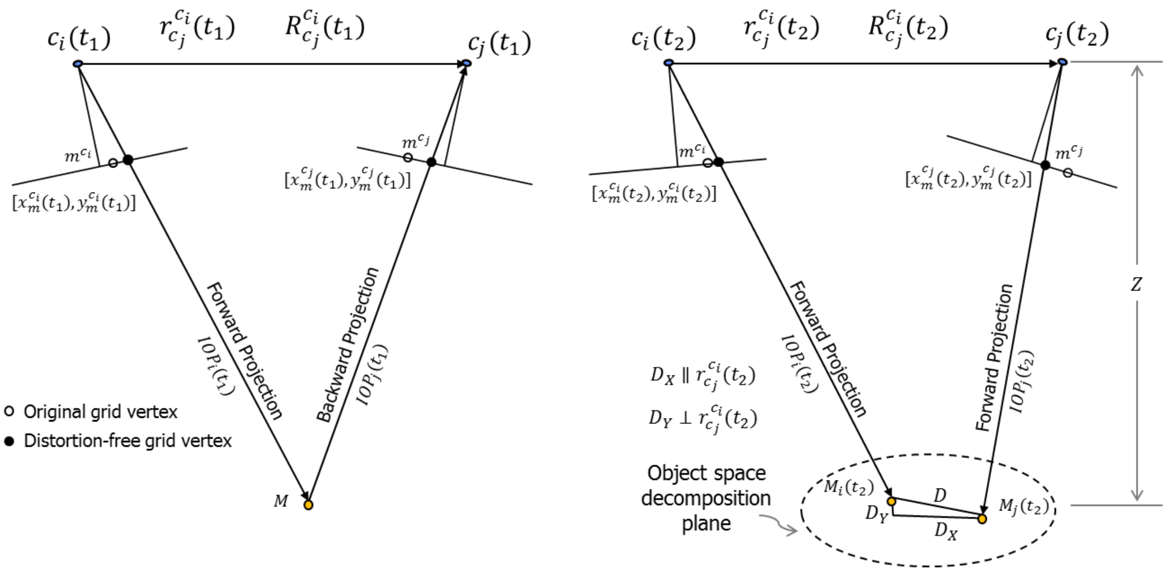

(a) (b)

Figure 4: Illustration of method 2 (object space parallax in image units): forward and backward projections for the first epoch (a), and forward projections for the second epoch (b) (Habib et al., 2014)

$$\delta x = D_X \cdot \bar{c}/Z \qquad \delta y = D_Y \cdot \bar{c}/Z \tag{2}$$

The implementation of Method 2 is more complex than the one for Method 1. However, this approach comprehensively considers the variations in the IOPs of both cameras in a stereo pair as well as any changes in the CMPs relating the two camera stations.

3.3 Method 3: variation in the normalized image coordinates

This method directly evaluates the image space impact caused by changes in the system calibration parameters. This is achieved through the generation of two sets of image coordinates normalized according to epipolar geometry. The first set of normalized image coordinates is generated using the first set of system calibration parameters, and correspondingly, the second set of image coordinates is generated using the second set of calibration parameters (see Figure 5). The parallax values for the x and y components are then computed for both t_1 and t_2 according to Equation (3). Finally, the RMSE for the x and y components is computed based on the differences shown in Equation (4):

$$p_{x^n}(t) = x^{c_i^n}(t) - x^{c_j^n}(t) \qquad p_{y^n}(t) = y^{c_i^n}(t) - y^{c_j^n}(t) \tag{3}$$

$$\delta p_{x^n} = p_{x^n}(t_2) - p_{x^n}(t_1) \qquad \delta p_{y^n} = p_{y^n}(t_2) - p_{y^n}(t_1) \tag{4}$$

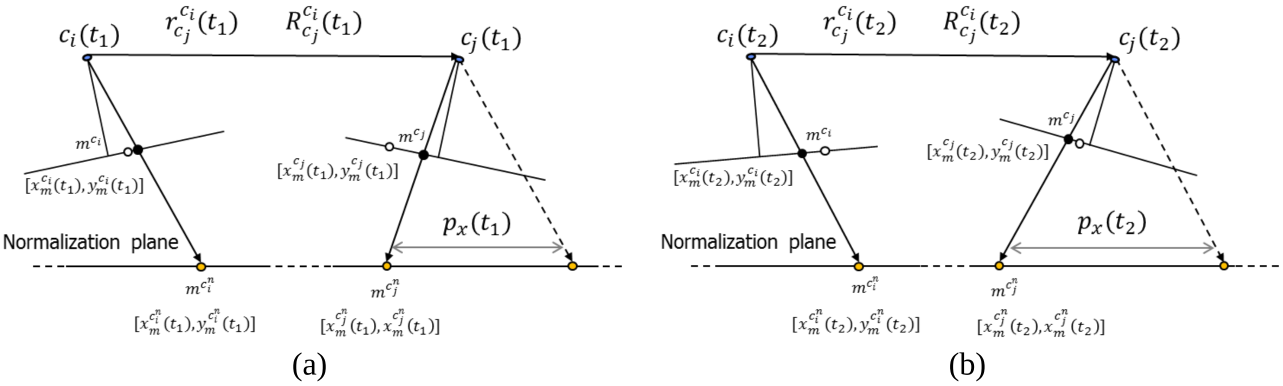

Figure 5: Partial illustration of method 3 (variation in the normalized image coordinates): side view for the image coordinate normalization at one epoch (a); changes in the imaging geometry, the normalized image coordinates, and the resultant x-parallax at another epoch (b) (Habib et al., 2014)

While this method consideres the variations in the IOPs of the involved cameras, it does not fully consider the variations in the CMPs between the two calibration sessions. More specifically, while variations in the rotational relationship and the orientation of the baseline between the two cameras stations would be detected, any changes to the magnitude (or the extent) of the baseline would not be correctly represented in the computed δp_{x^n} and δp_{y^n} values.

4. EXAMPLE SYSTEM SETUPS

In this research project, digital close range photogrammetric systems consisting of multiple cameras were used in a structural laboratory in order to perform precise deflection measurements. There were eight digital cameras employed in a typical photogrammetric system setup. The make and model for the cameras was Canon EOS 1000D / Rebel XS DSLR. The lenses used were of the Canon EF-S 18-55 mm f/ 3.5-5.6 zoom line. Each camera had a 10.1 mega pixel complementary metal oxide semiconductor (CMOS) solid state sensor (Canon Inc., 2008). The cameras were mounted on a steel frame via tripod heads with three degrees of freedom. The tripod heads were used to point the cameras towards the specimen of interest. After the cameras were focused on the specimen surface, the motion blur/vibration reduction, automatic focus, and sensor cleaning functions of the cameras were disabled.

Two different types of setups are shown in this section. In the first one (see Figure 6a), the camera system was suspended from an overhanging metal frame. This configuration was chosen so that the system can observe the top surface of a concrete beam while it was being deformed by a hydraulic actuator. In the second example system setup (see Figure 6b), the cameras were fixed to a metal frame, which was standing upright. This was the preferred orientation of the system because the surfaces of interest were the flange sides of a truss girder (Joulani, 2016; Joulani et al., 2016). In both setup examples, the multi-camera systems were calibrated in-situ by using a portable 2D test field. Note that the IOPs and CMPs were solved for simultaneously.

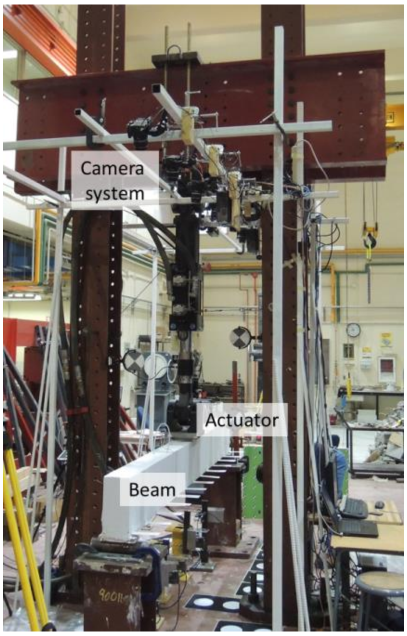

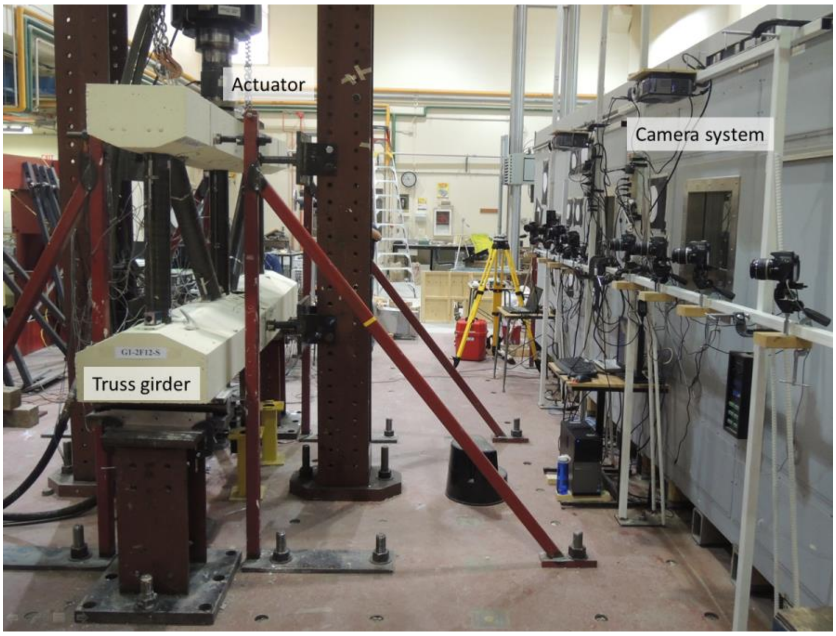

Figure 6: Suspended camera system setup (also showing the hydraulic actuator and the concrete beam specimen) (a); upright camera system setup (also showing the hydraulic actuator and the truss girder specimen) (b)

5. EXPERIMENTAL RESULTS

This section presents experimental results related to the proposed multi-camera system stability analysis methodologies. First, changes to the IOPs and CMPs of a particular system calibration session are added or simulated in order to verify the performance of the three system stability methods. Then, the most general method is used to assess the stability of a system in a long-term (e.g., multiple days) and a short-term (e.g., a few hours) scenarios. It is necessary to explore such system behaviour in order to decide how frequently to calibrate the system used.

5.1 Simulation of changes in the IOPs and CMPs

In order to test the developed tool for system stability analysis, a simulation test was executed. First, the same set of system calibration parameters was compared against itself. Then, changes in the system calibration parameters were made one at a time. In particular, the biases listed in Table 2 were introduced to each odd-numbered camera in the eight-camera system. The magnitudes of the applied biases were chosen as to cause noticeable system instability or RMSE values greater than one pixel for most of the cases. Note that this was done for testing purposes and that in reality the changes in the calibration parameters may not be as large as the chosen biases.

Table 2: Biases applied to the test set of system calibration parameters

Parameter symbol	Biases with units	Parameter description
x_p	+50 µm	x-component of the principal point offset
y_p	+50 µm	y-component of the principal point offset

c	+100 µm	principal distance
k_1	+5x10^{-5} mm^{-2}	first radial lens distortion coefficient
k_2	+5x10^{-7} mm^{-4}	second radial lens distortion coefficient
p_1	+1x10^{-5} mm^{-1}	first decentring lens distortion coefficient
p_2	+1x10^{-5} mm^{-1}	second decentring lens distortion coefficient
b_X	+5 mm	X-component of the positional offset
b_Y	+5 mm	Y-component of the positional offset
b_Z	+5 mm	Z-component of the positional offset
b_ω	+0.1°	ω rotational offset
b_φ	+0.1°	φ rotational offset
b_κ	+0.1°	κ rotational offset

The RMSEs or the effects in image space resultant from the simulated biases in the IOPs and CMPs are listed in Table 3. Two camera pairs are shown – Cams 3 & 4, and Cams 4 & 5, where Cam 3 and Cam 5 were the cameras, which had the above biases added to. Note that in the former pair, Cam 3 is the first camera, c_i, while in the latter pair, Cam 5 is the second camera, c_j, as per the notation used in this paper.

5.1.1 Method 1 vs. 2 comparison

As previously mentioned, Method 1, i.e., combination of forward and backward projections, ignores any changes in the IOPs for the first camera when deriving the stability analysis measure. This could be clearly seen at the IOP change instances under the Cams 3 & 4 column of Method 1 in Table 3. The Cam 4 & 5 column and all CMP change instances for Method 1 check with Method 2 reasonably well (e.g., the differences present were 1/5 of a pixel or less for most cases). Between the two, Method 2 should be the system stability method of choice unless the cameras in the system are stable and variations in the system calibration parameters only exist in the CMPs.

Table 3: Comparison between the system stability analysis methods by simulating changes in the IOPs and CMPs

Parameters / RMSEs	Method 1 Total RMSE [px]		Method 2 Total RMSE [px]		Method 3 Total RMSE [px]	
Cam pairs	Cams 3 & 4	Cams 4 & 5	Cams 3 & 4	Cams 4 & 5	Cams 3 & 4	Cams 4 & 5
None	0.00	0.00	0.00	0.00	0.00	0.00
Δx_p	0.00	8.76	8.83	8.96	8.90	8.98
Δy_p	0.00	8.76	8.82	8.95	8.84	8.91
Δc	0.00	5.25	6.18	5.43	4.46	5.47
Δk_1	0.00	4.85	2.84	4.95	2.91	5.03
Δk_2	0.00	5.15	2.17	5.17	2.23	5.26
Δp_1	0.00	0.27	0.18	0.28	0.19	0.29
Δp_2	0.00	0.16	0.13	0.17	0.13	0.17
Δb_X	10.57	10.51	11.05	10.75	0.15	0.57
Δb_Y	10.62	10.52	10.89	10.75	10.91	10.69

Δb_Z	3.15	3.01	3.40	3.12	4.48	4.02
Δb_ω	6.86	6.94	7.04	7.10	7.05	7.07
Δb_φ	6.70	7.18	7.01	7.36	7.27	7.39
Δb_κ	1.72	2.10	1.76	2.15	1.77	2.14

5.1.2 Method 3 vs. 2 comparison

As previously mentioned, Method 3, i.e., variation in the normalized image coordinates, does not fully consider changes in the CMPs. More specifically, it only detects changes in the rotational relationship between two camera stations, but ignores changes in the magnitude or extent of the baseline. Again, this problem can be seen in the CMP change instances under Method 3 in Table 3. While changes in the rotational CMPs, b_ω, b_φ and b_κ, can be detected in both Method 2 and Method 3 equally well, this is not true for the positional CMPs. Namely, the b_X change in the positional CMPs, i.e., the one primarily along the baseline of the cameras, is detected by Method 2, but goes unnoticed by Method 3. The IOP change instances between the two methods check reasonably well. Again, between the two, Method 2 should be the system stability method of choice as it works as expected in the most general case.

5.2 System stability analysis for a multi-day experiment

This subsection aims at analyzing the long-term stability behaviour of the overhanging system shown in Figure 6a. The system was used over the course of several days, and the system calibration parameters from three of the days were compared using Method 2. Table 4 lists the results for the Day 1 vs. Day 2, and the Day 2 vs. Day 3 system calibration parameters. No particular trend can be seen; however, the total RMSE values for some of the camera pairs are over one pixel. Due to these differences, it is recommended that more frequent system calibrations should be performed. For example, a system calibration should be added at the end of each day when data were collected. Also, when 3D object space reconstruction is performed, the set of calibration parameters used should be the one closest to the time the data for the object(s)/surface(s) of interest was acquired.

Table 4: Check for system stability during a multi-day experiment (overhanging system)

Cam pairs / RMSEs	RMSE x [px]		RMSE y [px]		Total RMSE [px]	
Days	Day 1 vs. Day 2	Day 2 vs. Day 3	Day 1 vs. Day 2	Day 2 vs. Day 3	Day 1 vs. Day 2	Day 2 vs. Day 3
Cams 1 & 2	0.37	0.69	0.52	0.60	0.64	0.92
Cams 2 & 3	0.35	0.70	0.96	0.75	1.02	1.02
Cams 3 & 4	0.24	0.54	0.37	0.13	0.44	0.56
Cams 4 & 5	0.84	0.45	0.64	0.17	1.05	0.48
Cams 5 & 6	1.25	0.31	1.23	0.52	1.75	0.60
Cams 6 & 7	1.05	0.39	0.27	0.60	1.09	0.71
Cams 7 & 8	0.84	2.25	0.71	0.86	1.10	2.41

5.3 Same-day system stability analysis

This subsection aims at analyzing the short-term stability behaviour of the upright system shown in Figure 6b. This system had to be calibrated for an experiment, which lasted less than a day. Three calibration data sets were acquired, namely before the experiment commenced (labelled as "pre"), a few hours later during a break (labelled as "mid"), and after the end of the experiment (labelled as "post"). Table 5 shows the results from the Pre vs. Mid and Mid vs. Post system stability analysis using Method 2. Again, no particular trend can be seen. The only worrisome instability was present in the pair Cams 7 & 8. Since the impact on the pair Cams 6 & 7 was much less, the instability must have come from Cam 8. Nevertheless, the reconstruction process would not be negatively impacted by a single unstable camera due to the built-in redundancy in the multiple light ray intersection. However, it would still be recommended to examine the environment around the camera in question, and make sure no foreign objects, such as wires or cables, are causing the instability.

Table 5: Check for system stability during an experiment lasting less than a day (upright system)

Cam pairs / RMSEs	RMSE x [px]		RMSE y [px]		Total RMSE [px]	
Experiment phases	Pre vs. mid	Mid vs. post	Pre vs. mid	Mid vs. post	Pre vs. mid	Mid vs. post
Cams 1 & 2	0.79	0.16	0.55	0.23	0.96	0.28
Cams 2 & 3	0.36	0.36	0.17	0.56	0.39	0.66
Cams 3 & 4	0.13	0.21	0.17	0.35	0.21	0.41
Cams 4 & 5	0.14	0.12	0.77	0.31	0.79	0.33
Cams 5 & 6	0.19	0.15	0.50	0.19	0.53	0.24
Cams 6 & 7	0.60	0.50	0.40	0.46	0.72	0.68
Cams 7 & 8	1.37	0.89	0.73	0.50	1.55	1.02

6. CONCLUSIONS AND FUTURE WORK

This paper presented three methods for performing stability analysis of a multi-camera system. The three methods handle IOPs and CMPs from different calibration sessions, and use simulated image space grids to yield a measure of the changes in the reconstructed object space in image space units. Given the outcome from the simulated data in the experimental results, in the most general case, Method 2 yields the most realistic measure of the (in)stability in a system with multiple cameras. However, if insignificant changes are expected for the IOPs of the first camera or the extent of the lever arm between the two camera stations, Method 1 and Method 3 also produce similar results. In addition, real world examples were given for both short term and long term system stability analysis scenarios related to system setups in a structural laboratory. Based on the results from the system stability analysis, it was possible to give recommendations on either the required frequency of calibration or on mitigating existing instability.

Future work for this project would involve developing a stability analysis method based on an object space simulation, so that the procedure is not limited to a pairwise relationship between two camera stations. In addition, testing wide angle prime lenses, switching to mirrorless cameras, or designing custom-made camera mounts in order to improve the camera and system stability could be considered.

ACKNOWLEGEMENTS

The authors would like to thank Dr. El-Badry and his team in civil engineering for providing us with the experimental environment, Dr. Hervé Lahamy and Jeremy Steward for assisting with the system setup and the data acquisition, and Dr. Eunju Kwak and Mehdi Mazaheri Tehrani for their help with the software.

REFERENCES

Canon Inc., 2008. EOS Rebel XS / EOS 1000D Instruction Manual.

Detchev, I., Habib, A., Chang, Y.-C., 2011. Image Matching and Surface Registration for 3D Reconstruction of a Scoliotic Torso. Geomatica 65, 175–187. doi:10.5623/cig2011-026

Detchev, I., Habib, A., El- Badry, M., 2013. Dynamic beam deformation measurements with off-the-shelf digital cameras. Journal of Applied Geodesy 7, 147–157. doi:10.1515/jag-2012-0052

Detchev, I., Habib, A., Mazaheri, M., Melia, A., 2015. Long Term Stability Analysis for a Multi-Camera Photogrammetric System, in: 2015 ASPRS Annual Conference. Tampa, FL.

Fraser, C.S., 1997. Digital camera self-calibration. ISPRS Journal of Photogrammetry and Remote Sensing 52, 149–159. doi:10.1016/S0924-2716(97)00005-1

Habib, A., Detchev, I., Kwak, E., 2014. Stability Analysis for a Multi-Camera Photogrammetric System. Sensors 14, 15084–15112. doi:10.3390/s140815084

Habib, A.F., Morgan, M.F., 2005. Stability analysis and geometric calibration of off-the-shelf digital cameras. Photogrammetric Engineering & Remote Sensing 71, 733–741.

Habib, A.F., Morgan, M.F., 2003. Automatic calibration of low-cost digital cameras. Optical Engineering 42, 948–955. doi:doi:10.1117/1.1555732

Habib, A.F., Pullivelli, A.M., Morgan, M.F., 2005. Quantitative measures for the evaluation of camera stability. Optical Engineering 44, 33605. doi:doi:10.1117/1.1872840

Harvey, E.S., Shortis, M.R., 1998. Calibration stability of an underwater stereo-video system: implications for measurement accuracy and precision. Marine Technology Society Journal 32, 3–17.

Harvey, E.S., Shortis, M.R., 1996. A system for stereo-video measurement of sub-tidal organisms. Marine Technology Society Journal 29, 10–22.

Joulani, P., 2016. Static and Fatigue Behaviour of Hybrid FRP-Concrete Two-Panel Truss Girders Reinforced with Double-Headed Glass FRP Bars (MSc Thesis). Department of Civil Engineering, University of Calgary, Calgary, Canada.

Joulani, P., El-Badry, M., Moravvej, M., 2016. Static Load Behaviour of Hybrid FRP-Concrete Two-Panel Truss Girders Reinforced with Double-Headed GFRP Bars, in: 5th International Structural Specialty Conference (ISSC-V). Presented at the The Canadian Society for Civil Engineering (CSCE), London, Ontario.

Kwak, E., Detchev, I., Habib, A., El-Badry, M., Hughes, C., 2013. Precise Photogrammetric Reconstruction Using Model-Based Image Fitting for 3D Beam Deformation Monitoring. Journal of Surveying Engineering 139, 143–155. doi:10.1061/(ASCE)SU.1943-5428.0000105

Lichti, D.D., 2008. A method to test differences between additional parameter sets with a case study in terrestrial laser scanner self-calibration stability analysis. ISPRS Journal of Photogrammetry and Remote Sensing 63, 169–180. doi:10.1016/j.isprsjprs.2007.08.001

Lichti, D.D., Habib, A., Detchev, I., 2009. An Object-space Simulation Method for Low-cost Digital Camera Stability Testing. Photogrammetric Engineering & Remote Sensing 75, 1407–1414.

Lichti, D.D., Sharma, G.B., Kuntze, G., Mund, B., Beveridge, J.E., Ronsky, J.L., 2015. Rigorous Geometric Self-Calibrating Bundle Adjustment for a Dual Fluoroscopic Imaging System. IEEE Transactions on Medical Imaging 34, 589–598. doi:10.1109/TMI.2014.2362993

Rau, J.-Y., Habib, A.F., Kersting, A.P., Chiang, K.-W., Bang, K.-I., Tseng, Y.-H., Li, Y.-H., 2011. Direct Sensor Orientation of a Land-Based Mobile Mapping System. Sensors 11, 7243–7261. doi:10.3390/s110707243

Remondino, F., El-Hakim, S.F., Gruen, A., Zhang, L., 2008. Turning images into 3-D models. IEEE Signal Processing Magazine 25, 55–64. doi:10.1109/MSP.2008.923093

Rieke-Zapp, D., Tecklenburg, W., Peipe, J., Hastedt, H., Haig, C., 2009. Evaluation of the geometric stability and the accuracy potential of digital cameras — Comparing mechanical stabilisation versus parameterisation. ISPRS Journal of Photogrammetry and Remote Sensing 64, 248–258. doi:10.1016/j.isprsjprs.2008.09.010

Shortis, M.R., Bellman, C.J., Robson, S., Johnston, G.J., Johnson, G.W., 2006. Stability of zoom and fixed lenses used with digital SLR cameras, in: The International Archives of the Photogrammetry, Remote Sensing and Spatial Information Sciences. Presented at the ISPRS Commission V Symposium, Dresden, Germany, pp. 285–290.

Shortis, M.R., Beyer, H.A., 1997. Calibration stability of the Kodak DCS420 and 460 cameras, in: SPIE Videometrics V. Presented at the Optical Science, Engineering and Instrumentation ’97, pp. 94–105.

Shortis, M.R., Miller, S., Harvey, E.S., Robson, S., 2000. An analysis of the calibration stability and measurement accuracy of an underwater stereo-video system used for shellfish surveys. Geomatics Research Australasia 73, 1–24.

Shortis, M.R., Ogleby, C.L., Robson, S., Karalis, E.M., Beyer, H.A., 2001. Calibration modeling and stability testing for the Kodak DC200 series digital still camera, in: SPIE Videometrics and Optical Methods for 3D Shape Measurement. San Jose, CA, pp. 148–153.

Shortis, M.R., Robson, S., Beyer, H.A., 1998. Principal Point Behaviour and Calibration Parameter Models for Kodak DCS Cameras. The Photogrammetric Record 16, 165–186. doi:10.1111/0031-868X.00119

Tommaselli, A.M.G., Galo, M., de Moraes, M.V.A., Marcato, J., Caldeira, C.R.T., Lopes, R.F., 2013. Generating Virtual Images from Oblique Frames. Remote Sensing 5, 1875–1893. doi:10.3390/rs5041875

BIOGRAPHICAL NOTES

Dr. Ivan Detchev received his BScE (First Division) in geomatics engineering from the University of New Brunswick in 2007, and his MSc and PhD in digital imaging system from the University of Calgary in 2010 and 2016, respectively. His MSc thesis was on the 3D reconstruction of scoliotic torsos, and prototypes of the implemented system are currently being used in the Alberta Children's Hospital (Calgary, Canada) and in the IWK Health Centre (Halifax, Canada). His PhD dissertation was in close range photogrammetry and it was related to image-based fine-scale infrastructure monitoring. Dr. Detchev also has industry experience in surveying and remote sensing. His previous employers include G. R. Williams Land Surveying Ltd. (Vancouver, BC) and Pacific Geomatics Ltd. (Surrey, BC). He is currently a tenure-track instructor in surveying and mapping in the Department of Geomatics Engineering at the University of Calgary.

CONTACTS

Ivan Detchev, Ph.D.
Department of Geomatics Engineering
University of Calgary
2500 University Dr. NW
Calgary
CANADA
Tel. + 1-403-220-4978
Fax + 1-403-284-1980
Email: i.detchev@ucalgary.ca
Web site: https://schulich.ucalgary.ca/profiles/ivan-detchev